Simple description of odd-A nuclei around the critical point of the spherical to axially deformed shape phase transition

Yu Zhang, Feng Pan, Yu-Xin Liu, Yan-An Luo, and J. P. Draayer

Phys. Rev. C **84**, 034306 — Published 6 September 2011

DOI: 10.1103/PhysRevC.84.034306

A simple description of odd-A nuclei around the critical point of the spherical to axially deformed shape phase transition

Yu Zhang,[1] Feng Pan,[1,2] Yu-Xin Liu,[3,4] Yan-An Luo,[5] and J. P. Draayer[2]

[1]*Department of Physics, Liaoning Normal University, Dalian 116029, China*
[2]*Department of Physics and Astronomy, Louisiana State University, Baton Rouge, LA 70803-4001, USA*
[3]*Department of Physics and the National Key Laboratory of Nuclear Physics and Technology, Peking University, Beijing 100871, China*
[4]*Center of Theoretical Nuclear Physics, National Laboratory of Heavy Ion Accelerator, Lanzhou 730000, China*
[5]*School of Physics, Nankai University, Tianjin 300071, China*

(Dated: August 16, 2011)

An analytically solvable model, X(3/ $2j+1$), is proposed to describe odd-A nuclei near the X(3) critical point. The model is constructed based on a collective core described by the X(3) critical point symmetry coupled to a spin-j particle. A detailed analysis of the spectral patterns for $j = 1/2,\ 3/2$ cases is provided to illustrate dynamical features of the model. Through comparing the theory with experimental data and results of other models, it is found that the X(3/ $2j+1$) model can be taken as a simple yet very effective scheme to describe those odd-A nuclei with an even-even core at the critical point of the spherical to axially deformed shape phase transition.

PACS numbers: 21.60.Fw, 21.60.Ev, 05.70.Fh, 21.10.Re

I. Introduction

Recently, critical point symmetries [1–5] have attracted considerable attention, since they provide benchmark results for the study of even-even nuclei as they undergo a transition between two different phases (shapes) [6–22]. In particular, the critical point of the spherical to γ-unstable shape transition [1], called E(5), and the critical point from the spherical to axially deformed shape [2], called X(5), have been confirmed by experiment [23–26]. In view of their successful application in helping to understand even-even systems, it seems critical point symmetries in odd-A systems warrant further investigation. And since the low-lying structures of two adjacent nuclei with more or less than one neutron or proton should be driven by similar collective considerations, the critical point symmetries observed in even-even systems should also be evident in the adjacent odd-A nuclei. The first case of a critical point Bose-Fermi symmetry, called E(5/4) [27], was developed by Iachello to describe, analytically, the γ-soft critical point E(5) configuration coupled to a $j = 3/2$ particle. ^{135}Ba was suggested as an empirical example of E(5/4) symmetry, with a report of a detailed analysis given in [28]. While these results show significant agreement between theory and experiment, there are also some differences. Another critical point Bose-Fermi symmetry, called E(5/12) [29], was developed by Alonso, Arias, and Vitturi, who extended the case of the E(5/4) symmetry with a spin-j particle into the multi-j case with $j = 1/2,\ 3/2,\ 5/2$. Both the E(5/4) and E(5/12) models were developed to describe odd-A nuclei near even-even nuclei that display the E(5) critical point symmetry [1]; that is, nuclei in the spherical to γ-unstable transitional region. As the X(5) symmetry seems well confirmed in experiment [2], it provides a better test for exploring effects of the X(5) critical point symmetry in odd-A nuclei near the even-even partners at the X(5) critical point. Very recently, in the same spirit as the E(5/4) and E(5/12) examples, an X(5/ $2j$+1) model that coupled a spin-j particle to the X(5) symmetry core was advanced [30].

In this article, we propose an exactly solvable model, called X(3/ $2j$+1), based on the X(3) critical point symmetry [5]. Although the original X(5/ $2j$+1) model was designed to describe the similar physical situation, it can only be solved analytically within an approximation as shown in [30], where the coupling strength between the even-even core and single-j particle is taken as the same value for different odd-A nuclei. The purpose of the present study is three fold. One is to provide a simple solvable model scheme to describe odd-A nuclei near the critical point of the spherical to axially deformed shape phase transition. Another is to investigate the dynamical features of the model in a variety of parameter situations. The third is to test the validity of the model through widely comparing the theory with experimental data and results of other models.

In Section II, the X(3/ $2j$+1) model will be constructed by coupling the X(3) core [5] with a spin-j particle. In Section III, as specific examples, the case with j=1/2 and $j = 3/2$, namely X(3/2) and X(3/4), will be provided to illustrate the spectral patterns of the model. Typical quantities in a variety of parameter situations will be analyzed. In Section IV, comparisons of the X(3/ $2j$+1) results to the corresponding experimental data will be made. A summary is given in Section V.

II. Construction of the X(3/ $2j$+1) model

First recall that similar to the Nilsson model [31], the E(5/4) model [27] is constructed by considering the case of coupling a collective core described by the E(5) symmetry [1] with a spin $j = 3/2$ particle via a five-dimensional "spin-orbit" interaction $\hat{\Sigma}\circ\hat{\Lambda}$, which is a scalar of the Spin(5) or SO(5) group [27, 32]. The corresponding Hamiltonian can be written as

$$H_{\mathrm{E(5/4)}} = H_{\mathrm{E(5)}} + g(\beta)[2\hat{\Sigma}\circ\hat{\Lambda} + 5/2]\,, \tag{1}$$

where $H_{\mathrm{E(5)}}$ is the E(5) Hamiltonian for the even-even core. A similar coupling scheme was also adopted to develop the X(5/ $2j$+1) model in [30]. We follow the paradigm of the E(5/4) model to construct the X(3/ $2j$+1) model by introducing a spin-orbit interaction $f(\beta)(\hat{L}\cdot\hat{j})$, where $\hat{L}$ is the orbital angular momentum operator of the X(3) core, $\hat{j}$ is the spin operator of the particle, and $f(\beta)$ is the coupling strength. It is clear that $\hat{L}\cdot\hat{j}$ is only a scalar of the $\mathrm{SU}_J(2)$ group in this case, where J is the total angular momentum of the system coupled from the orbital angular momentum L of the core with the spin j of the odd particle, similar to a Nilsson type model where the odd-particle is coupled to the even-even core. Then, the Hamiltonian of the X(3/ $2j$+1) model is written as

$$H = H_{\mathrm{X(3)}} + f(\beta)[\hat{L}\cdot\hat{j} + b\hbar^2]\,, \tag{2}$$

where b is an adjustable parameter, and $H_{\mathrm{X(3)}}$ is the Hamiltonian of the X(3) even-even core. It will be shown that the case with the parameter $b \neq 0$ in Eq. (2) seems better in describing the corresponding experimental data. As shown in Eq. (1), a similar situation appears in the E(5/4) model [27], where the parameter b is set to be 5/2. The explicit Bohr Hamiltonian of (2) is

$$\begin{aligned} H = &-\tfrac{\hbar^2}{2B}[\tfrac{1}{\beta^2}\tfrac{\partial}{\partial\beta}\beta^2\tfrac{\partial}{\partial\beta} + \tfrac{1}{3\beta^2}(\tfrac{1}{\sin\theta}\tfrac{\partial}{\partial\theta}\sin\theta\tfrac{\partial}{\partial\theta} + \tfrac{1}{\sin^2\theta}\tfrac{\partial^2}{\partial\phi^2})] \\ &+V(\beta) + f(\beta)[\hat{L}\cdot\hat{j} + b\hbar^2]\,, \end{aligned} \tag{3}$$

in which B is the inertia parameter, and the potential $V(\beta)$ is taken to be an infinite square well with

$$V(\beta) = \begin{cases} 0\,, & \beta \leq \beta_W\,, \\ \infty\,, & \beta > \beta_W\,. \end{cases} \tag{4}$$

It should be noted that the potential in the X(3) model [5] is only a function of the β variable since the γ variable is frozen at $\gamma = 0$. Thus solving the X(3/2j+1) model becomes a three-dimensional problem, while the E(5/4) model and X(5/2j+1) model are five-dimensional. The β-dependent coupling strength $f(\beta)$ is taken to be $f(\beta) = \frac{f}{B\beta^2}$, where f is a real parameter, which is the same as that adopted in the E(5/4) model [27]. As shown in the following, the model is exactly solvable with such choice of $f(\beta)$.

By solving the eigen-equation $H\Psi(\beta,\theta,\phi,\chi) = E\Psi(\beta,\theta,\phi,\chi)$, it is shown that the eigenfunction may be constructed by coupling the collective core part with the single-particle state χ_{j,m_j} in the spherical form as

$$\Psi_{LjJM_J}(\beta,\theta,\phi,\chi) = F(\beta) \sum_{M_L m_j} \langle L, M_L; j, m_j | J, M_J\rangle Y_{LM_L}(\theta,\phi)\chi_{j,m_j}\,, \tag{5}$$

where $Y_{LM_L}(\theta,\phi)$ is the spherical harmonic function. Thus, the spin-orbit interaction can be further expressed as

$$\frac{f}{B\beta^2}\hat{L}\cdot\hat{j} = \frac{f}{2B\beta^2}[\hat{J}\cdot\hat{J} - \hat{L}\cdot\hat{L} - \hat{j}\cdot\hat{j}] \tag{6}$$

with $\hat{J} = \hat{L} + \hat{j}$.

After introducing the reduced energies ϵ=$2BE/\hbar^2$ and reduced potential u=$2BV/\hbar^2$, one can write the Schrödinger equation in separable variable form in the standard way

$$-(\frac{1}{\sin\theta}\frac{\partial}{\partial\theta}\sin\theta\frac{\partial}{\partial\theta} + \frac{1}{\sin^2\theta}\frac{\partial^2}{\partial\phi^2})Y_{LM}(\theta,\phi) = L(L+1)Y_{LM}(\theta,\phi)\,, \tag{7}$$

$$\{-\frac{1}{\beta^2}\frac{\partial}{\partial\beta}\beta^2\frac{\partial}{\partial\beta} + \frac{1}{\beta^2}[(\frac{1}{3} - f)L(L+1) + fJ(J+1) - fj(j+1) + 2fb] + u(\beta)\}F(\beta) = \epsilon F(\beta)\,. \tag{8}$$

As mentioned above, $V(\beta)$=$\frac{\hbar^2}{2B}u(\beta)$ is an infinite well potential. Substituting $\varphi = \beta^{1/2}F(\beta)$ and $z = \beta\sqrt{\epsilon}$, one can transform Eq. (8) inside the well into a Bessel equation

$$\varphi'' + \frac{\varphi'}{z} + [1 - \frac{v^2}{z^2}]\varphi = 0 \tag{9}$$

with

$$v = [(\frac{1}{3} - f)L(L+1) + fJ(J+1) - fj(j+1) + 2fb + \frac{1}{4}]^{1/2}\,. \tag{10}$$

It is clear that the contribution of the quantum number L to the order of the Bessel equation is completely canceled when $f = 1/3$, which is a situation similar to that of the E(5/4) model [27], where the contribution of the quantum number τ of the SO(5) group to the order of the Bessel function is canceled when $k = 1$. Considering the boundary condition $\varphi(\beta_W) = 0$, one gets the eigenvalues

$$\epsilon_{s,LjJ} = (k_{s,LjJ})^2, \quad k_{s,LjJ} = \frac{z_{s,LjJ}}{\beta_W}\,, \tag{11}$$

where $z_{s,LjJ}$ is the s-th zero of the Bessel function $J_v(z)$ with $z = k_{LjJ}\beta$. While the relevant eigenfunctions

$$F_{s,LjJ}(\beta) = c_{s,LjJ}\beta^{-1/2}J_v(k_{s,LjJ}\beta)\,, \tag{12}$$

where $c_{s,LjJ}$ is the normalization constant to be determined from the condition

$$\int_0^{\beta_W} F^2_{s,LjJ}(\beta)\beta^2 d\beta = 1\,. \tag{13}$$

B(E2) transition rates can be calculated by taking the quadrupole operator $T^{(E2)} = T^{\rm c} + T^{\rm f}$, where $T^{\rm c}$ only operates on the core part, and $T^{\rm f}$ operates on the single-particle part. For simplicity, we take $T^{(E2)} = T^{\rm c}$ in the model which is the same as that used in [30]. The specific form of the quadrupole operator is given by

$$T^{\rm c}_u = t\beta[D^2_{u,0}(\theta_1,\theta_2,\theta_3)\cos\gamma + \frac{1}{\sqrt{2}}\left(D^2_{u,2}(\theta_1,\theta_2,\theta_3) + D^2_{u,-2}(\theta_1,\theta_2,\theta_3)\right)\sin\gamma], \tag{14}$$

where $\theta_1,\ \theta_2$, and θ_3 denote the Euler angles, and t is a scale factor. For $\gamma = 0$, only the $D^2_{u,0}(\theta_1,\theta_2,\theta_3)$ term survives.

III. Spectral patterns of the X(3/ 2j+1) model

Similar to other critical point Bose-Fermi symmetry models [27, 29, 30], this model is called X(3/ $2j$+1) model since it is built from the X(3) core coupled to a spin-j particle with $m_j = -j, \cdots,\ j$. The spectrum generated from different critical point symmetry models may be characterized by the "critical" orders of the corresponding Bessel functions associated with their solutions. In Table I, we list the "critical" orders of various critical point Bose-Fermi symmetry models for odd-A systems as well as the related critical point symmetry models for even-even systems studied up till now. It can be seen from Table I that the "critical" orders become model parameter dependent for odd-A systems, from which the spectra of odd-A systems will thus become more complex than those of even-even cases. The coupling strength parameters in these models for odd-A systems are not arbitrarily adjustable, which has not been emphasized in our previous study [30]. As shown in Table I, the coupling strength f in the X(n/$2j$+1) model with $n = 3$ or 5 should satisfy

$$f[L(L+1) + j(j+1) - J(J+1)] < \frac{1}{3}L(L+1) \tag{15}$$

to ensure the ground state spin is $J = j$, which requires the "critical" order of the Bessel function associated with the ground state to be less than those associated with excited states. In addition, $f \geq 0$ is assumed to ensure that the energy levels with the same L not decrease with increasing values of J, which is consistent with most situations observed in experiments. Since the lowest excited state is the one with the quantum number $J = |L - j|$ and $L = 2$ for a given j, the above conditions require

$$\begin{cases} 0 \leq f < \frac{1}{3j} & \text{for } j < 2, \\ 0 \leq f < \frac{1}{2j+2} & \text{for } j > 2, \end{cases} \tag{16}$$

which provides with the restricted condition for the parameter f in the model. Specifically, the restricted condition (16) requires $f < 2/3$ for $j = 1/2$, $f < 2/9$ for $j = 3/2$, $f < 1/7$ for $j = 5/2$, $f < 1/9$ for $j = 7/2$, $f < 1/11$ for $j = 9/2$, and $f < 1/13$ for $j = 11/2$. As a result, The larger the j value, the weaker the coupling strength between the even-even core and the particle. Anyway, only a very narrow range for the parameter f can be chosen from to fit for the odd-A nuclei, which thus limits the arbitrariness of the $X(n/2j{+}1)$ model predictions. Similar restriction to the coupling strength parameter also occurs in the E(5/4) model. The coupling strength parameter k in the E(5/4) model should satisfy $k > -4$ to ensure the quantum numbers $(\tau, J){=}(0, 3/2)$ corresponding to those of the ground state because the core is coupled with only a $j = 3/2$ particle [27]. Actually, $k = 1$ was taken in [27] and $k = -1/2$ in [28], which both satisfy the restriction $k > -4$.

To study spectral patterns of the X(3/ $2j$+1) model, we take $j = 1/2$ and $j = 3/2$ cases as examples. Some low-lying energy levels and related B(E2) transition rates are calculated, of which the results are shown in Fig. 1. It should be noted that both energy levels and transition rates of the model can be calculated analytically up to an overall scale after fixing the parameters f and b.

To test the roles of the coupling strength parameter f and the spin j in the spectrum of the X(3/$2j$+1), we have set $b = 0$ in Fig. 1. As shown in Fig. 1, an obvious feature of the X(3/2) model is that predicted B(E2) values for transitions with $\Delta J = 2$ are much larger than those with $\Delta J = 1$ for both the strong coupling case with $f = 1/3$ and the weak coupling case with $f = 1/30$, except those of the lowest three transitions with comparable strengths in every panel. Further numerical calculations show that this feature is independent of the parameter b. In addition, the energy levels with the same L are approximately degenerate in the weak coupling case ($f = 1/30$), while the degeneracy is broken in the strong coupling case ($f = 1/3$). Anyway, for fixed nonzero L, energy levels become much

TABLE I: The "critical" orders of typical critical point symmetry models, where τ, τ_1^F and (τ_1, τ_2) are the quantum numbers of $O^B(5)$, $O^F(5)$ and $O^{BF}(5)$, respectively [27, 29, 32].

Critical point symmetry	"Critical" order
E(5)	$\sqrt{\tau(\tau+3)+\frac{9}{4}}$
E(5/4)	$\sqrt{(1-k)\tau(\tau+3)+k[\tau_1(\tau_1+3)-\frac{7}{4}+b]+\frac{9}{4}}$
E(5/12)	$\sqrt{(1-k)\tau(\tau+3)+k[\tau_1(\tau_1+3)+\tau_2(\tau_2+1)]+(k'-k)\tau_1^F(\tau_1^F+3)]+\frac{9}{4}}$
X(5)	$\sqrt{\frac{L(L+1)}{3}+\frac{9}{4}}$
X(5/2j+1)	$\sqrt{(\frac{1}{3}-f)L(L+1)+fJ(J+1)-fj(j+1)+\frac{9}{4}}$
X(3)	$\sqrt{\frac{L(L+1)}{3}+\frac{1}{4}}$
X(3/2j+1)	$\sqrt{(\frac{1}{3}-f)L(L+1)+fJ(J+1)-fj(j+1)+\frac{1}{4}+2fb}$

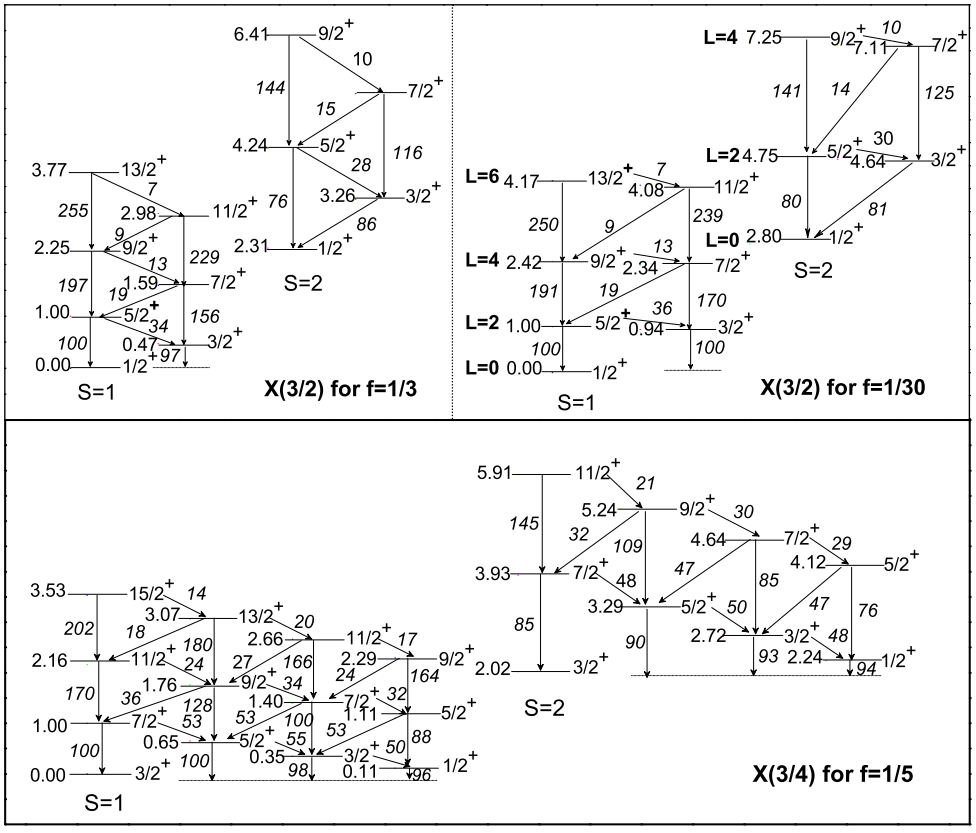

FIG. 1: The spectrum of the X(3/2) model with $f = 1/3$ and $f = 1/30$ corresponding to the case of the X(3) even-even core coupled to an $s_{1/2}$, and the X(3/4) model with $f = 1/5$ corresponding to the case of the core coupled to a $d_{3/2}$ particle. For $p_{1/2}$ or $p_{3/2}$ case, all parities should be reversed. In our calculation, the parameter b in Eq (3) has been taken as zero, and all energy levels are normalized to the energy of the first $(j+2)_1^+$ excited state and the B(E2) transition values are normalized to that of the $B(E2; (j+2)_1^+ \to j_1^+)$.

denser with increasing of the spin j. For instance, there are only two states in the X(3/2) model if $L \neq 0$, while there are four states in the X(3/4) model. Therefore, the spectrum in the X(3/4) model becomes more complex than that in the X(3/2) model. The main feature of B(E2) transition rates in the X(3/4) model is similar to that in the X(3/2) model. In Fig. 1, we only list a case with $f = 1/5$ for the X(3/4) model because f should be less than 2/9 for $j = 3/2$ as discussed previously. In a weaker coupling case with $0 < f \ll 1/5$ in the X(3/4) model, the spectral character is

also similar to that in the X(3/2) model with weak coupling.

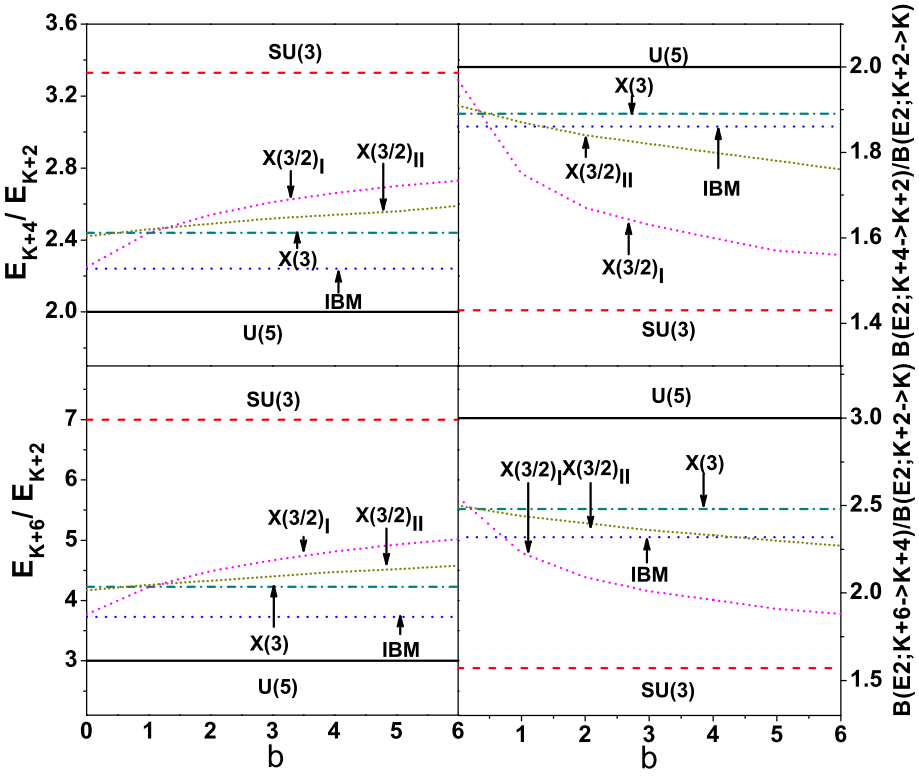

FIG. 2: Typical energy ratios and B(E2) ratios as functions of the parameter b in different models. For odd-A systems, $X(3/2)_I$ and $X(3/2)_{II}$ curves represent the results obtained from the X(3/2) model for the strong coupling case ($f = 1/3$), and the weak coupling case ($f = 1/30$), respectively. For even-even systems, X(3) curves denotes the results obtained from the X(3) model [5], while U(5), SU(3), and IBM curves represent the results calculated from the U(5) limit, SU(3) limit, and the critical point of U(5)-SU(3) phase transition in the interaction boson model with $N = 10$, respectively, where the results characterized by U(5), SU(3), and IBM are calculated with the Hamiltonian $H = c[(1-\xi)n_d - \frac{\xi}{4N}(Q^\chi \cdot Q^\chi)]$ used in [15]. In addition, $K = 0$ for even-even systems and $K = 1/2$ for odd-A systems.

Another issue is the influence of the parameter b, which is also involved in the E(5/4) symmetry as shown in Table I, but it has been set to 5/2 in [27] and 0 in [32]. In the X(3/2j+1) model, b will be treated as an adjustable parameter in fitting experimental results. As mentioned above, the X(3/2j+1) model is used to describe the spherical to axially deformed shape phase transition in odd-A system. The similar situation in even-even system has been widely studied in the interacting boson model (IBM) [33]. To make the influence of the parameter b clear, we take the X(3/2) model as an example to compare typical energy ratios and B(E2) ratios calculated from the related models in Fig. 2, where $b \geq 0$ is assumed because the spectrum of the X(3/2j+1) model with negative b becomes too soft as in comparison with experimental results. It is clearly shown in Fig. 2 that the results for both the strong-coupling case represented by $X(3/2)_I$ and the weak-coupling one characterized with $X(3/2)_{II}$ monotonously move towards those of the SU(3) limit with increasing value of b, which indicates that the larger the b value, the more rigid the system becomes. In addition, the quantities in the strong-coupling case vary with b faster than those in the weak-coupling case when b is small, but they almost keep as constants when $b > 5$. All of them with the variation of b keep in between the results of the U(5) limit (spherical phase) and those of the SU(3) limit (axially deformed phase).

IV. Comparison with experimental results

Generally, spectra of odd-A nuclei are more complex than those of even-even nuclei, especially for those undergoing shape phase transitions. In the following, we take the odd-A nuclei with the nearest even-even nuclei around the X(3) critical point as experimental candidates of the X(3/2j+1) symmetry. Specifically, because ^{186}Pt lies near the X(3) critical point [5], it is reasonable to take ^{187}Au [34] as an experimental candidate since the valence proton outside the even-even core in this case may occupy the $3s_{1/2}$ orbit, and the ground state of ^{187}Au is just $1/2^+_1$. In addition, since ^{154}Gd, ^{104}Mo, ^{152}Sm, and ^{150}Nd are also well described by the X(3) or X(5) model [25, 35–37], their nearest

odd-proton partners, namely, ^{155}Tb [38], ^{105}Tc [39], ^{153}Eu [40], and ^{151}Pm [41] may be taken as the X(3/2j+1) symmetry candidates. According to the shell model, the single valence proton in these odd-A nuclei may occupy the $2d_{3/2}$, $2p_{3/2}$, $2d_{5/2}$, and $2d_{5/2}$ orbits, respectively. The J^π of the ground state in the corresponding odd-A nucleus is just $3/2^+$, $3/2^-$, $5/2^+$, and $5/2^+$, which agree with the corresponding experimental observations. In Fig. 3-7, only the level schemes of ^{187}Au, ^{155}Tb, ^{105}Tc, ^{153}Eu, and ^{151}Pm, consisting of the lowest positive (negative) parity states with $L = 0, 2, 4, 6$, are chosen to be compared with results calculated from the X(3/2j+1) model.

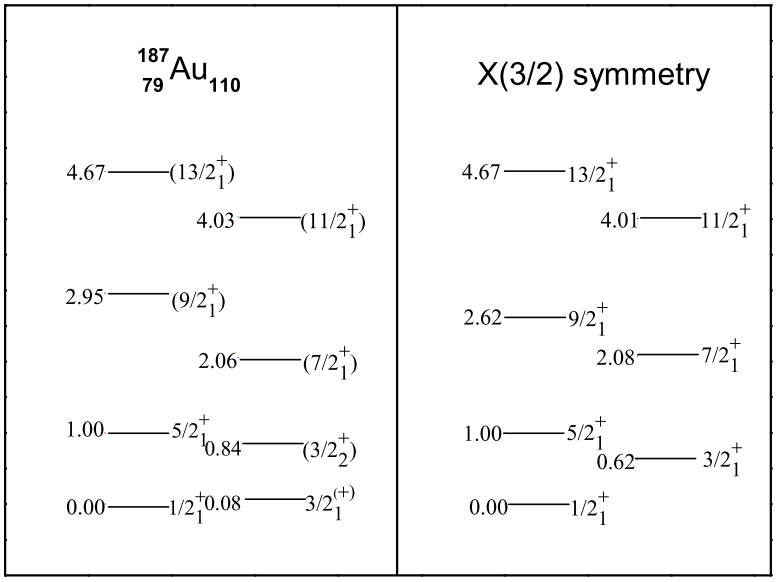

FIG. 3: The ground state band of ^{187}Au [34] and spectrum of the X(3/2) model with $f = 1/5$ and $b = 3$. The state in parentheses means the corresponding quantum number has not been confirmed in the experiment.

It is shown in Fig. 3 that the theory agrees well with the experimental results of ^{187}Au [34] except for the $3/2^+_1$ state. The experimental $3/2^+_1$ state is nearly degenerate with the $1/2^+_1$ ground state which may come from a single-particle excitation because the $3s_{1/2}$ orbit is near the adjacent $2d_{3/2}$ orbit. A similar situation also occurs in ^{189}Au [30] and ^{135}Ba [28]. In this work, the $3/2^+_2$ state of ^{187}Au is assigned to be the $3/2^+_1$ state in the X(3/2) model. As shown in Fig. 4, the X(3/4) model also agrees well with the experimental results of ^{155}Tb [38], which was also chosen as the X(5/2j+1) model candidate in [30]. The present X(3/2j+1) results seem little better in quantity than those of the X(5/2j+1) model shown in [30]. There are also two obvious exceptions between the experiment and the theory. Firstly, the collective $3/2^+_2$ and $1/2^+_1$ levels based on the ground state in the theory are not observed in experiment. Two levels with ($1/2^+$, $3/2^+$, $5/2^+$) at 508.395 keV and ($3/2^+$, $5/2^+$, $7/2^+$) at 517.542 keV observed in the experiment [38] are noticeably too higher to be the two states predicted based on the ground state in the theory. Secondly, the $9/2^+_1$ and $13/2^+_1$ levels from the X(3/4) model are also noticeably higher than those observed in experiment. For ^{105}Tc, as shown in Fig. 5, the agreement between the experimental data [39] and those calculated in the X(3/4) model is generally good, especially in the lower part of the spectrum, except that some relative high collective states including $9/2^-_2$, $11/2^-_2$, and $13/2^-_1$ are not observed in experiment. It should be noted that negative parity states of ^{105}Tc known in experiment [39] have all been shown in Fig. 5. There are still several spin and parity undetermined levels between $11/2^-_1$ and $15/2^-_1$ reported in [39] not shown in Fig. 5, which may be the $9/2^-_2$, $11/2^-_2$, and $13/2^-_1$ levels predicted in the model, but need to be confirmed. Similar to the case shown in Fig. 4, the collective $1/2^-_1$ level is also not observed in experiment. In addition, the candidates of $3/2^-_2$ in experiment, which is marked with $(3/2^-, 5/2^-)$ as shown in Fig. 5, is higher than that calculated from the X(3/4) model. As for $j = 5/2$ case, the results of the X(3/6) model also grossly agree with the experimental results of ^{153}Eu [40] and ^{151}Pm [41] shown in

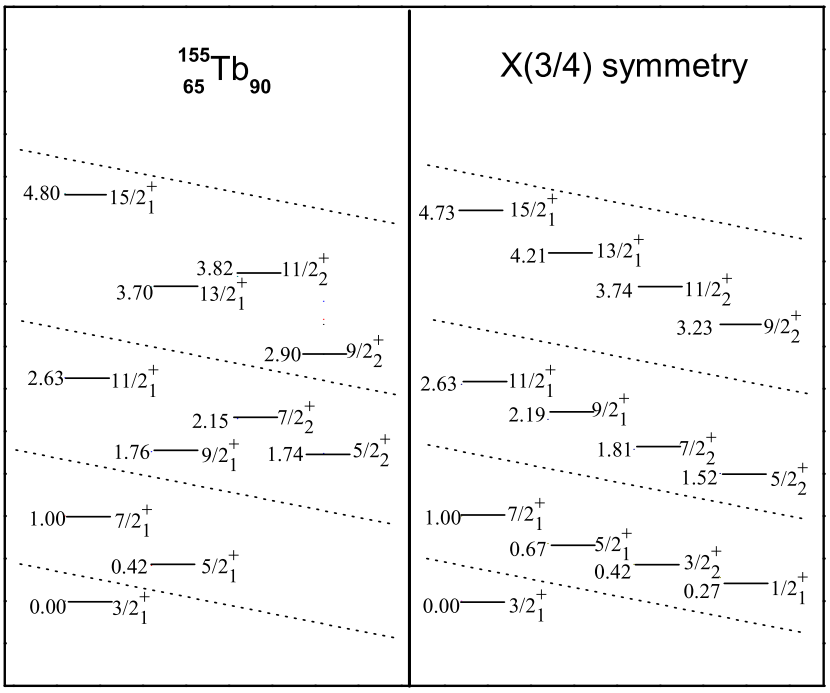

FIG. 4: Some low-lying levels of ^{155}Tb [38] with those calculated from the X(3/2j+1) model with $j = 3/2$, $f = 1/7$ and $b = 11$, where the lowest positive parity with $L = 0, 2, 4, 6$, are shown.

Fig. 6 and Fig. 7. In addition, the collective $9/2^+_3$ level for ^{151}Pm is not observed in the experiment as shown Fig. 7. The collective $9/2^+_3$ level, according to the theory, should not be higher than that of $17/2^+_1$ for $j = 5/2$ case according to the similar situation shown in Fig. 6. Thus, it will be interesting to verify whether the level marked with (?), which is the only level with unknown spin and parity below the $17/2^+_1$ level in the experiment [41], is just the $9/2^+_3$ level. All in all, it can be seen from Fig. 3−7 that the energy ratios $E_{(j+4)_1}/E_{(j+2)_1}$ and $E_{(j+6)_1}/E_{(j+2)_1}$ in experiment are not only excellently consistent with the results of the X(3/2j+1) model, but also in between the corresponding results of the U(5) limit and those of the SU(3) limit shown in Fig 2.

TABLE II: Some B(E2) values (in w.u.) with parameter t fitted by $B(E2; 7/2^+_1 \to 5/2^+_1)$ obtained from the X(3/6) model compared with available experimental data of ^{153}Eu [40], and those for the X(3/4) model with t fitted by $B(E2; 5/2^+_1 \to 3/2^+_1)$ compared with experimental data of ^{155}Tb [38]. In our calculation, the $5/2^+_3$ and $3/2^+_2$ states in the X(3/6) model are assigned to be the $5/2^+_2$ and $3/2^+_1$ states of ^{153}Eu as shown in Fig. 6, of which the related B(E2) values fitted by the theory are given in the first column under the $X(3/6)$ table head. It should be noted that the parameter f and b are the same as those used for Fig 4 and Fig. 6.

$J^\pi_i \to J^\pi_f$	^{153}Eu	X(3/6)	$J^\pi_i \to J^\pi_f$	^{153}Eu	X(3/6)	$J^\pi_i \to J^\pi_f$	^{155}Tb	X(3/4)
$7/2^+_1 \to 5/2^+_1$	300(21)	300	$5/2^+_{2,3} \to 7/2^+_1$	4(4)	14, 176	$5/2^+_1 \to 3/2^+_1$	88(13)	88
$9/2^+_1 \to 7/2^+_1$	170(40)	173	$3/2^+_{1,2} \to 7/2^+_1$	1.1	0.9, 193	$7/2^+_1 \to 5/2^+_1$	≥ 39	44
$9/2^+_1 \to 5/2^+_1$	97(8)	303	$5/2^+_{2,3} \to 5/2^+_1$	0.5(7)	0, 296	$7/2^+_1 \to 3/2^+_1$	≥ 28	89
$5/2^+_{2,3} \to 3/2^+_{1,2}$	138(9)	147, 29	$3/2^+_{1,2} \to 5/2^+_1$	1.3(9)	0, 293	$9/2^+_1 \to 7/2^+_1$	$\sim$	30

Since only a spin-orbit type interaction $f(\beta)[\hat{L} \cdot \hat{j} + b\hbar^2]$ is introduced to describe the interaction between the

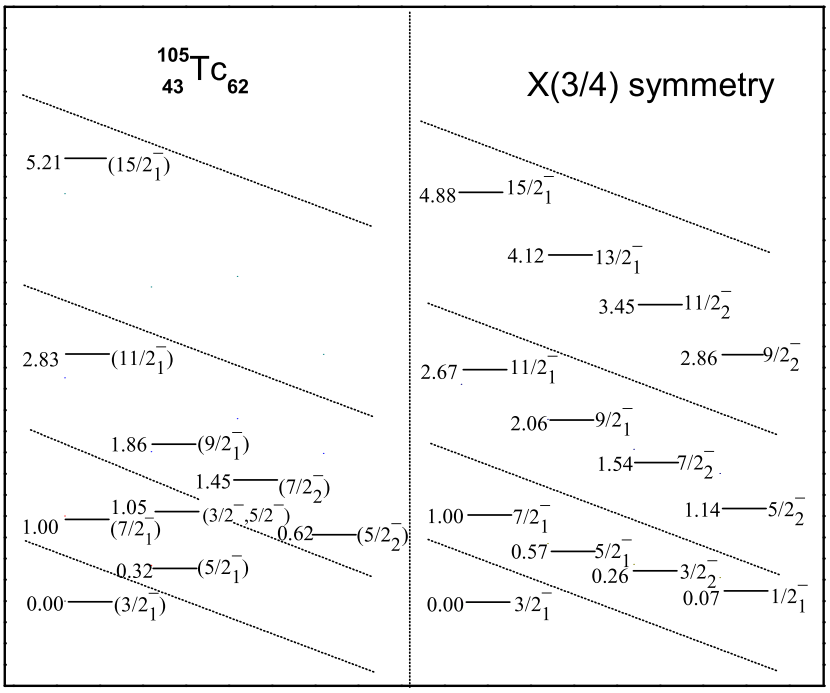

FIG. 5: The low-lying levels of ^{105}Tc [39] and those calculated from the X(3/2j+1) model with $j = 3/2$, $f = 1/5$ and $b = 19$, where the lowest negative parity with $L = 0, 2, 4, 6$, are shown. The state in parentheses means the corresponding quantum number has not been confirmed in the experiment.

core and a single valence nucleon in the X(3/2j+1) model, the energy levels for fixed L will increase with J according to Eq. (6). But the energy levels in experiments do not change so regularly as in the theory. Therefore, differences in quantity between experiment and the theory always exist as seen from Fig. 6 and Fig. 7. Another discrepancy between the theory and experiment is that some low collective levels predicted in the X(3/2j+1) model are not observed in experiment, such as the $j = 5/2$ case shown in Fig. 6 and Fig. 7. As shown in Fig. 4−7, these experimentally unobserved levels are often very low in energy and close to the ground state in the theory. If one choose the coupling-parameter f larger than the restricted condition allowed, for example, taking $f = 1/3 > 1/7$, those experimentally unobserved levels, such as $5/2_2^+$, $3/2_1^+$ and $1/2_1^+$ shown in the X(3/6) model, will be lower than the $5/2_1^+$ levels and thus become nonphysical. More realistic interactions such as the quadrupole-type interaction and interactions among multi-j single-particle orbits may be necessary to improve the theory, from which a better description of low-lying structure of odd-A nuclei may be reached. These possible extensions for the theory will be studied in our future work.

To further check the X(3/2j+1) symmetry, some B(E2) values, which are sensitive to structures of wavefunctions, are taken to be compared with available experimental data, which are shown in Table II. As shown in Table II, it is impressive that the experimental results are well reproduced by the theory, especially for the noticeable difference between the strong transitions and the weak ones for ^{153}Eu. It should be noted that the B(E2) values of ^{153}Eu involved in $5/2_2^+$ and $3/2_1^+$ are far higher or lower than the corresponding ones with $5/2_2^+$ and $3/2_1^+$ in the X(3/6) model as shown in Table II. But the same results in experiments consist well with those calculated with $5/2_3^+$ and $3/2_2^+$ in the theory. Therefore, the B(E2) values further confirm that the $5/2_2^+$ and $3/2_1^+$ levels in experiment should correspond to the $5/2_3^+$ and $3/2_2^+$ respectively in the X(3/6) model as shown in Fig. 6.

V. Summary and Conclusions

In this paper, the X(3/ 2j+1) model is proposed for odd-A nuclei that neighbor even-even systems displaying characteristics of a spherical to axially deformed (shape) phase transition. Specifically, the model provides a simple

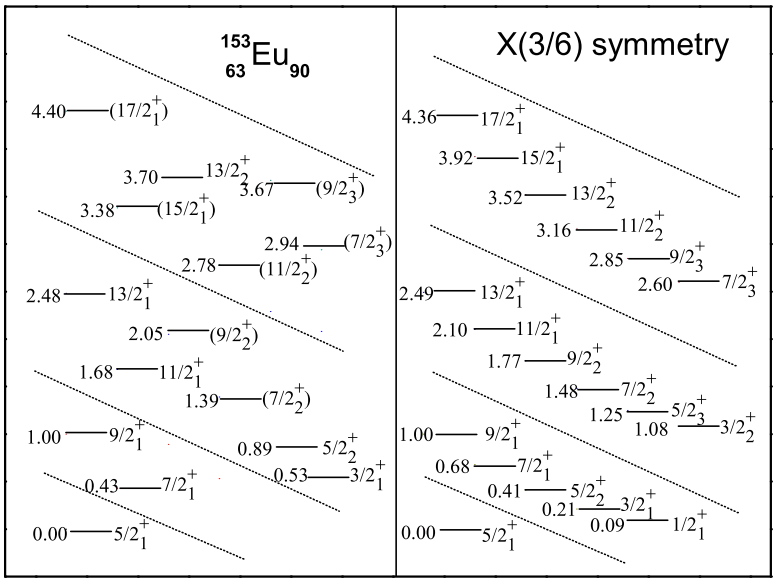

FIG. 6: The low-lying levels of ^{153}Eu [40] and those calculated from the X(3/2j+1) model with $j = 5/2$, $f = 1/8$ and $b = 10$, where the lowest positive parity with $L = 0, 2, 4, 6$, are shown. The state in parentheses means the corresponding quantum number has not been confirmed in the experiment.

and solvable framework to test the relevance of the X(3) critical point symmetry [5] in odd-A nuclei. The j=1/2 and j=3/2 cases were selected as specific examples to illustrate its typical spectral patterns. Comparison with other related models is also made. The results indicate that the X(3/ 2j+1) model can be used to describe the spherical to axially deformed phase transition in odd-A nuclei rather well. It is shown that ^{187}Au, ^{155}Tb, ^{105}Tc, ^{153}Eu, and ^{151}Pm may be possible X(3/ 2j+1) symmetry candidates as seen in terms of the band-head configurations and the structure of low-lying spectra. By-in-large the model results grossly agree with the corresponding experimental data. However, further work –experimental as well as theoretical, is needed to help unveil the role of the critical point symmetries in structure of nearby odd-A nuclei. In addition, a complete description of low-lying states of odd-A nuclei requires further extensions of the model. One extension may be made by considering the X(3) core coupled to multi-j single-particle states as done in the E(5/12) model [29]. A strong-coupling scheme of the X(3) core coupled with a set of deformed single-particle states may also be needed in contrast to the present treatment which is similar to the weak-coupling approximation. This follows because the interaction between the core and the single-particle is expected to be quite strong in the odd-A nuclei when the core is well-deformed. In addition, a detailed comparison of the X(3/ 2j+1) model with the interacting boson-fermion model [42–44] and the SD-pair shell model [45, 46] for odd-A nuclei would be interesting. Related work is in progress.

Acknowledgments

Support from the U.S. National Science Foundation (PHY-0500291 & OCI-0904874), the Southeastern Universities Research Association, the Natural Science Foundation of China (11005056 and 10775064), the Liaoning Education Department Fund (2007R28), the Doctoral Program Foundation of State Education Ministry of China

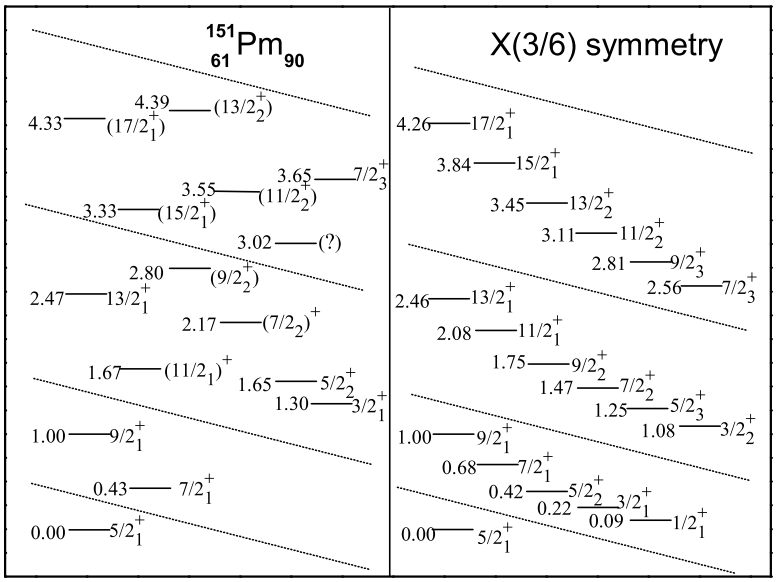

FIG. 7: The low-lying levels of ^{151}Pm [41] and those calculated from the X(3/2j+1) model with $j = 5/2$, $f = 1/8$ and $b = 8$, where the lowest positive parity with $L = 0, 2, 4, 6$, are shown. The state in parentheses means the corresponding quantum number has not been confirmed in the experiment, and the one marked with (?) means that the spin and parity of this state is still known in the experiment.

(20102136110002), and the LSU–LNNU joint research program (9961) is acknowledged.

[1] F. Iachello, Phys. Rev. Lett. **85**, 3580 (2000).
[2] F. Iachello, Phys. Rev. Lett. **87**, 052502 (2001).
[3] F. Iachello, Phys. Rev. Lett. **91**, 132502 (2003).
[4] D. Bonatsos, D. Lenis, D. Petrellis, and P. A. Terziev, Phys. Lett. **B 588**, 172-179 (2004).
[5] D. Bonatsos, D. Lenis, D. Petrellis, P. A. Terziev, and I. Yigitoglu, Phys. Lett. **B 632**, 238-242 (2006).
[6] J. N. Ginocchio, and M. W. Kirson, Phys. Rev. Lett. **44**, 1744 (1980).
[7] A. E. L. Dieperink, O. Scholten, and F. Iachello, Phys. Rev. Lett. **44**, 1747 (1980).
[8] D. H. Feng, R. Gilmore, and S. R. Deans, Phys. Rev. **C 23**, 1254 (1981).
[9] P. van Isacker and J. Q. Chen, Phys. Rev. **C 24**, 684 (1981).
[10] J. Jolie, P. Cejnar, R. F. Casten, S. Heinze, A. Linnemann, and V. Werner, Phys. Rev. Lett. **89**, 182502 (2002).
[11] F. Iachello and N. V. Zamfir, Phys. Rev. Lett. **92**, 212501 (2004).
[12] D. J. Rowe, Phys. Rev. Lett. **93**, 122502 (2004)
[13] D. J. Rowe, P. S. Turner, and G. Rosensteel, Phys. Rev. Lett. **93**, 232502 (2004).
[14] P. Cejnar, S. Heinze, and J. Dobeš, Phys. Rev. **C 71**, 011304(R) (2005).
[15] P. Cejnar, J. Jolie, and R. F. Casten, Rev. Mod. Phys. **80**, 2155 (2010).
[16] S. Dusuel, J. Vidal, J. M. Arias, J. Dukelsky, and J. E. García-Ramos, Phys. Rev. **C 72**, 064332 (2005).
[17] J. M. Arias, J. Dukelsky, J. E. García-Ramos, and J. Vidal, Phys. Rev. **C 75**, 014301 (2007).
[18] D. D. Warner and R. F. Casten, Phys. Rev. **C 28**, 1798 (1983).
[19] A. Leviatan, Phys. Rev. Lett. **77**, 818 (1996); **98**, 242502 (2007); A. Leviatan and P. van Isacker, Phys. Rev. Lett. **89**, 222501 (2002).
[20] Y. X. Liu, L. Z. Mu, and H. Wei, Phys. Lett. **B 633**, 49 (2006).
[21] Y. Zhang, Z. F. Hou, H. Chen, H. Wei, and Y. X. Liu, Phys. Rev. **C 78**, 024314 (2008).

[22] Y. Zhang, Z. F. Hou, and Y. X. Liu, Phys. Rev. **C 76**, 011305(R) (2007).
[23] R. F. Casten and N. V. Zamfir, Phys. Rev. Lett. **85**, 3584 (2000).
[24] R. M. Clark, et al., Phys. Rev. **C 69**, 064322 (2004).
[25] R. F. Casten and N. V. Zamfir, Phys. Rev. Lett. **87**, 052503 (2001).
[26] R. M. Clark, et al., Phys. Rev. **C 68**, 037301 (2003).
[27] F. Iachello, Phys. Rev. Lett. **95**, 052503 (2005).
[28] M. S. Fetea et al., Phys. Rev. **C 73**, 051301(R) (2006).
[29] C. E. Alonso, J. M. Arias, and A. Vitturi, Phys. Rev. Lett. **98**, 052301 (2007); Phy. Rev. **C 75**, 064316 (2007).
[30] Y. Zhang, F. Pan, Y. X. Liu, Z. F. Hou, and J. P. Draayer, Phys. Rev. **C 82**, 034327 (2010).
[31] S. G. Nilsson and I. Ragnarsson, Shapes and Shells in Nuclear Structure (Cambridge University Press, Cambridge, England, 1995).
[32] M. A. Caprio and F. Iachello, Nucl. Phys. A **781**, 26-66 (2007).
[33] F. Iachello and A. Arima, *The Interacting Boson Model* (Cambridge University, Cambridge, England, 1987).
[34] M. S. Basunia, Nucl. Data Sheets **110**, 999 (2009).
[35] D. Tonev *et al.*, Phys. Rev. **C 69**, 034334 (2004).
[36] P. G. Bizzeti and A. M. Bizzeti-sona, Phys. Rev. **C 66**, 031301(R) (2002).
[37] R. Krücken *et al.*, Phys. Rev. Lett. **88**, 232501 (2002).
[38] C. W. Reich, Nucl. Data Sheets **104**, 1 (2005).
[39] D. De Frenne and E. Jacobs, Nucl. Data Sheets **105**, 775 (2005).
[40] R. G. Helmer, Nucl. Data Sheets **107**, 507 (2006).
[41] B. Singh, Nucl. Data Sheets **80**, 263 (1997).
[42] J. Jolie, S. Heinze, P. Van Isacker, and R. F. Casten, Phys. Rev. **C 70**, 011305(R) (2004).
[43] C. E. Alonso, J. M. Arias, L. Fortunato, and A. Vitturi, Phys. Rev. **C 72**, 061302(R) (2005).
[44] M. Böyükata, C. E. Alonso, J. M. Arias, L. Fortunato, and A. Vitturi, Phys. Rev. **C 82**, 014317 (2010).
[45] J. Q. Chen and Y. A. Luo, Nucl. Phys. **A 639**, 615 (1998).
[46] Y. A. Luo, Y. Zhang, X. F. Meng, F. Pan and J. P. Draayer, Phys. Rev. **C 80**, 014311 (2009).